Population receptive field analysis of the primary visual cortex complements perimetry in patients with homonymous visual field defects

Amalia Papanikolaou[a,b], Georgios A. Keliris[a,c,1], T. Dorina Papageorgiou[d], Yibin Shao[a], Elke Krapp[e], Eleni Papageorgiou[e,f], Katarina Stingl[e], Anna Bruckmann[e], Ulrich Schiefer[e,g], Nikos K. Logothetis[a,h], and Stelios M. Smirnakis[d,i]

[a]Max Planck Institute for Biological Cybernetics, 72076 Tuebingen, Germany; [b]Graduate School of Neural and Behavioural Sciences, International Max Planck Research School, 72076 Tuebingen, Germany; [c]Bernstein Center for Computational Neuroscience, 72076 Tuebingen, Germany; [d]Departments of Neuroscience and Neurology, Baylor College of Medicine, Houston, TX 77030; [e]Center for Ophthalmology, University Eye Hospital Tuebingen, 72076 Tuebingen, Germany; [f]Department of Ophthalmology, University of Leicester, Leicester Royal Infirmary, Leicester LE2 7LX, United Kingdom; [g]Competence Center "Vision Research," Faculty of Optics and Mechatronics, Aalen University of Applied Sciences, 73430 Aalen, Germany; [h]Division of Imaging Science and Biomedical Engineering, University of Manchester, Manchester M13 9PT, United Kingdom; and [i]Michael E. Debakey VA Medical Center, Houston, TX 77030

Edited by Brian A. Wandell, Stanford University, Stanford, CA, and approved February 25, 2014 (received for review September 13, 2013)

Injury to the primary visual cortex (V1) typically leads to loss of conscious vision in the corresponding, homonymous region of the contralateral visual hemifield (scotoma). Several studies suggest that V1 is highly plastic after injury to the visual pathways, whereas others have called this conclusion into question. We used functional magnetic resonance imaging (fMRI) to measure area V1 population receptive field (pRF) properties in five patients with partial or complete quadrantic visual field loss as a result of partial V1+ or optic radiation lesions. Comparisons were made with healthy controls deprived of visual stimulation in one quadrant ["artificial scotoma" (AS)]. We observed no large-scale changes in spared-V1 topography as the V1/V2 border remained stable, and pRF eccentricity versus cortical-distance plots were similar to those of controls. Interestingly, three observations suggest limited reorganization: (*i*) the distribution of pRF centers in spared-V1 was shifted slightly toward the scotoma border in 2 of 5 patients compared with AS controls; (*ii*) pRF size in spared-V1 was slightly increased in patients near the scotoma border; and (*iii*) pRF size in the contralesional hemisphere was slightly increased compared with AS controls. Importantly, pRF measurements yield information about the functional properties of spared-V1 cortex not provided by standard perimetry mapping. In three patients, spared-V1 pRF maps overlapped significantly with dense regions of the perimetric scotoma, suggesting that pRF analysis may help identify visual field locations amenable to rehabilitation. Conversely, in the remaining two patients, spared-V1 pRF maps failed to cover sighted locations in the perimetric map, indicating the existence of V1-bypassing pathways able to mediate useful vision.

cortical blindness | quadrantanopia | plasticity | retinotopy | hemianopia

Cortical damage of the visual pathway often results from posterior or middle cerebral artery infarcts, hemorrhages, and other brain injuries. The most common visual cortex lesions involve the primary visual cortex (V1), the chief relayer of visual information to higher visual areas. Damage to area V1 or its primary inputs leads to the loss of conscious vision in the corresponding region of the contralateral visual hemifield, producing a dense contralateral scotoma that often covers a hemifield (hemianopia) or a single visual field quadrant (quadrantanopia).

A much-debated issue is whether the adult V1 is able to reorganize after injury. Reorganization refers to long-term changes in the neuronal circuit (1) and generally requires the growth of new anatomic connections or a permanent change in the strength of existing connections. Several studies report significant remapping in area V1 of patients suffering from macular degeneration and other retinal lesions (2–12). The extent of this remapping has recently been called into question, however (1, 13–19). Less is known about how the visual system remaps to cover the visual field after injury to area V1 or its input projection from the lateral geniculate nucleus (LGN). Enlarged receptive fields have been found in areas surrounding chronic V1 lesions in cats (20–22), and visual point spread functions were seen to enlarge over time in the areas surrounding focal V1 lesions in kittens (23). Smaller, short-term changes (2 d after the lesion) have been reported as well (24). As expected, reorganization is more extensive in young animals (23, 25) compared with adults (26). A change in the balance between excitation and inhibition may underlie this functional reorganization (27–31).

In humans, V1 injury is typically followed by a brief period of spontaneous recovery, which rarely lasts beyond 6 mo (32). Whether this recovery is the result of true visual system plasticity or is related to the gradual resolution of perilesional edema and general clinical improvement of the patients is unclear. A recent study in an adult human subject suggested that large-scale reorganization occurs in area V1 after partial deafferentiation by an optic radiation lesion (33); however, quantitative measurements were not performed. To date, there has been no systematic study in humans investigating how spared V1 cortex covers the visual field after chronic V1 injury. The present work is an effort in this direction.

Significance

Partial damage of the primary visual cortex (V1), or damage to the white matter inputs to V1 (optic radiation), cause blindness in specific regions of the visual field. We use functional MRI to measure responses in individual patients with a localized, chronic V1 injury that resulted in blindness in a quarter of the visual field. The fMRI responses of patients and controls are generally similar, but in some patients differences from controls can be measured. Importantly, responses in spared early visual cortex are not always congruent with visual perception. Understanding how the properties of early visual areas respond to injury will lead to better strategies for visual rehabilitation.

Author contributions: A.P., G.A.K., U.S., N.K.L., and S.M.S. designed research; A.P., G.A.K., T.D.P., Y.S., E.K., E.P., K.S., A.B., and S.M.S. performed research; A.P. and T.D.P. analyzed data; and A.P., G.A.K., and S.M.S. wrote the paper.

Conflict of interest statement: U.S. serves as a consultant for Haag-Streit Inc., Köniz, Switzerland.

This article is a PNAS Direct Submission.

Freely available online through the PNAS open access option.

[1]To whom correspondence should be addressed. E-mail: georgios.keliris@tuebingen.mpg.de.

This article contains supporting information online at www.pnas.org/lookup/suppl/doi:10.1073/pnas.1317074111/-/DCSupplemental.

We used the population receptive field (pRF) mapping method (34) to study how spared area V1 covers the visual field after chronic injury in five adult human subjects suffering from partial or complete quadrantanopia. Our findings suggest that there is at best a limited degree of reorganization in the spared part of area V1 after partial V1 injury. Interestingly, the pattern of coverage of the visual field measured in spared V1 cortex by functional magnetic resonance imaging (fMRI) typically does not match predictions derived from perimetry maps. Identifying the patterns of mismatch and how they relate to the capacity of early visual areas to reorganize after injury will eventually allow the adoption of more rational strategies for visual rehabilitation.

Results

Retinotopic Mapping of Spared Area V1. We studied five patients with partial V1 or optic radiation lesions resulting in partial or complete quadrantanopia (Table S1) and examined how the adjacent spared area V1 organization changes after the injury. We expected that in the absence of significant reorganization, retinotopic organization in the spared-V1 cortex would remain unchanged compared with controls. The patient's lesions are described in detail in Fig. 1. In brief, patient P1 had a lesion of the right inferior calcarine cortex (Fig. 1 *A*, *a*), resulting in a superior quadrantanopic defect of the left visual field (Fig. 2 *A*, *b*). Patient P2 had a right superior quadrantanopia (Fig. 2 *A*, *c*) after sustaining a temporal optic radiation infarct of the left hemisphere. Patient P3 had a lesion of the left inferior calcarine region resulting in a central (<10° radius) right superior quadrantanopia (Fig. 2 *A*, *d*), which spread slightly into the inferior right quadrant. Patient P4 had a lesion of the left inferior calcarine cortex, resulting in a right superior quadrantanopia (Fig. 2 *A*, *e*). Patient P5 had a partial left superior quadrantanopia extending to the inferior quadrant across the horizontal meridian (Fig. 2 *A*, *f*), resulting from an infarct in the right midposterior temporoparietal region (Fig. 1 *A*, *e*).

We observed two general patterns in the five patients examined. In patients P1, P2, and P3, spared (i.e., not completely deafferented) area V1 seems to retain its "coarse" retinotopic

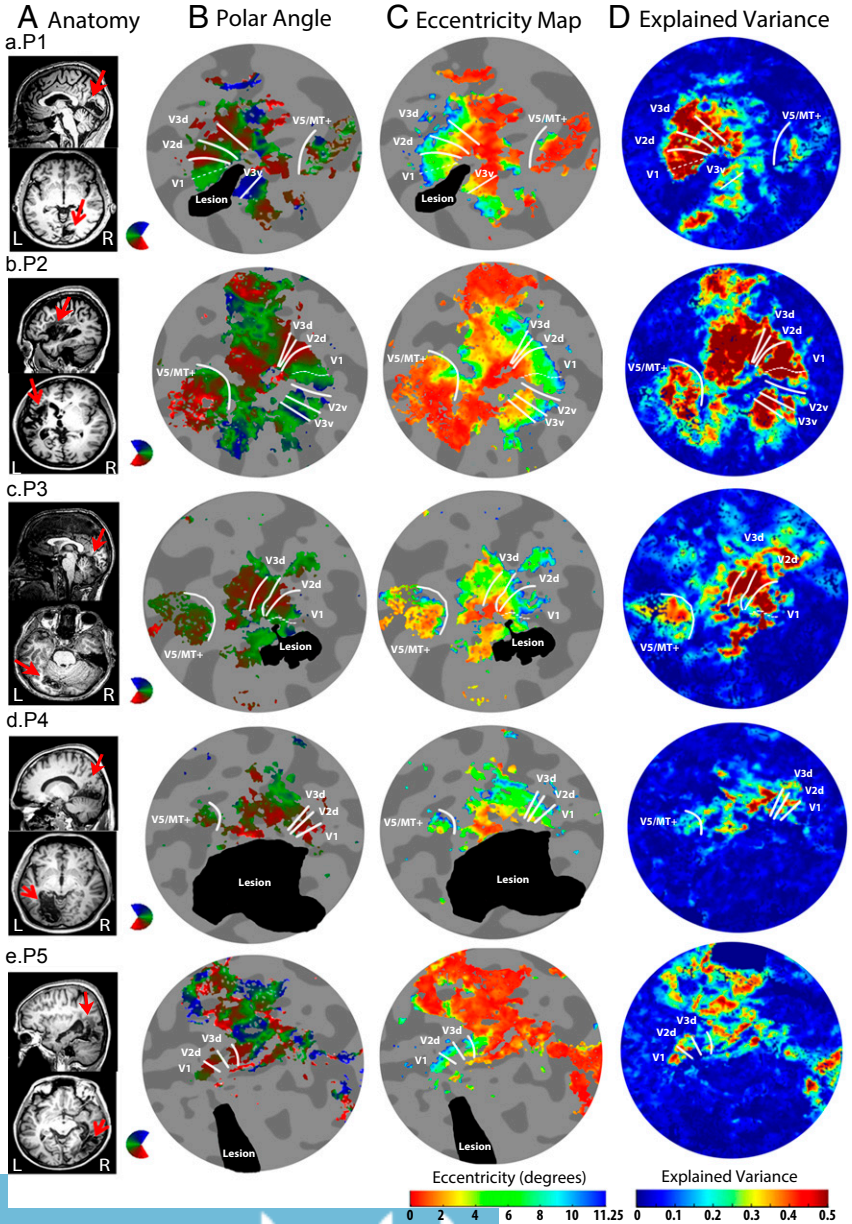

Fig. 1. Anatomic location of the lesion and retinotopic mapping. (*A*) Sagittal (*Upper*) and axial (*Lower*) slice showing each patient's anatomic lesion (a red arrow points to the lesion). Patient P1 had a lesion of the right inferior calcarine cortex involving the part of the V1 area inferior to the calcarine sulcus and the part of the extrastriate cortex corresponding to the ventral visual areas V2 and V3, with the foveal part of the vertical meridian at the border of ventral V3 and V4 spared. Patient P2 had a temporal optic radiation infarct of the left hemisphere located along the territory of the middle cerebral artery, sparing the gray matter of area V1 but deafferenting a significant portion of it by injuring the optic radiation. Patient P3 had a lesion of the left inferior calcarine cortex as a result of an ischemic event at the left inferior territory of the posterior cerebral artery, resulting in a right upper quadrantanopia. This lesion also involves part of the peripheral (>10° radius) area V1 superior to the calcarine, as well as extrastriate cortex corresponding to ventral visual areas V2, V3, and V4. Patient P4 had a lesion of the left inferior calcarine cortex caused by an infarct to the lower bank of the calcarine fissure. It involves left ventral area V1, left ventral extrastriate areas V2, V3, and V4, as well as part of the cortex near the fovea. Patient P5 had an infarct of the right midposterior temporoparietal lobes that damaged the temporal optic radiation and part of the parietal optic radiation. White matter tracts in the temporal lobe were affected, but deafferented V1 gray matter remained intact; the area corresponding to the anatomic lesion does not include early visual areas. (*B* and *C*) Polar angle (*B*) and eccentricity maps (*C*) overlaid on the flattened occipital lobe of the lesioned hemisphere for each patient. The lesioned area is colored black (Fig. S4 and *SI Materials and Methods*). (*D*) As expected, no significant activity was found inside the area of the lesion, as shown in the explained variance map. White contour lines indicate borders between visual areas. The dashed white line indicates the middle of the calcarine sulcus as identified by its anatomic localization (i.e., bottom of the calcarine sulcus).

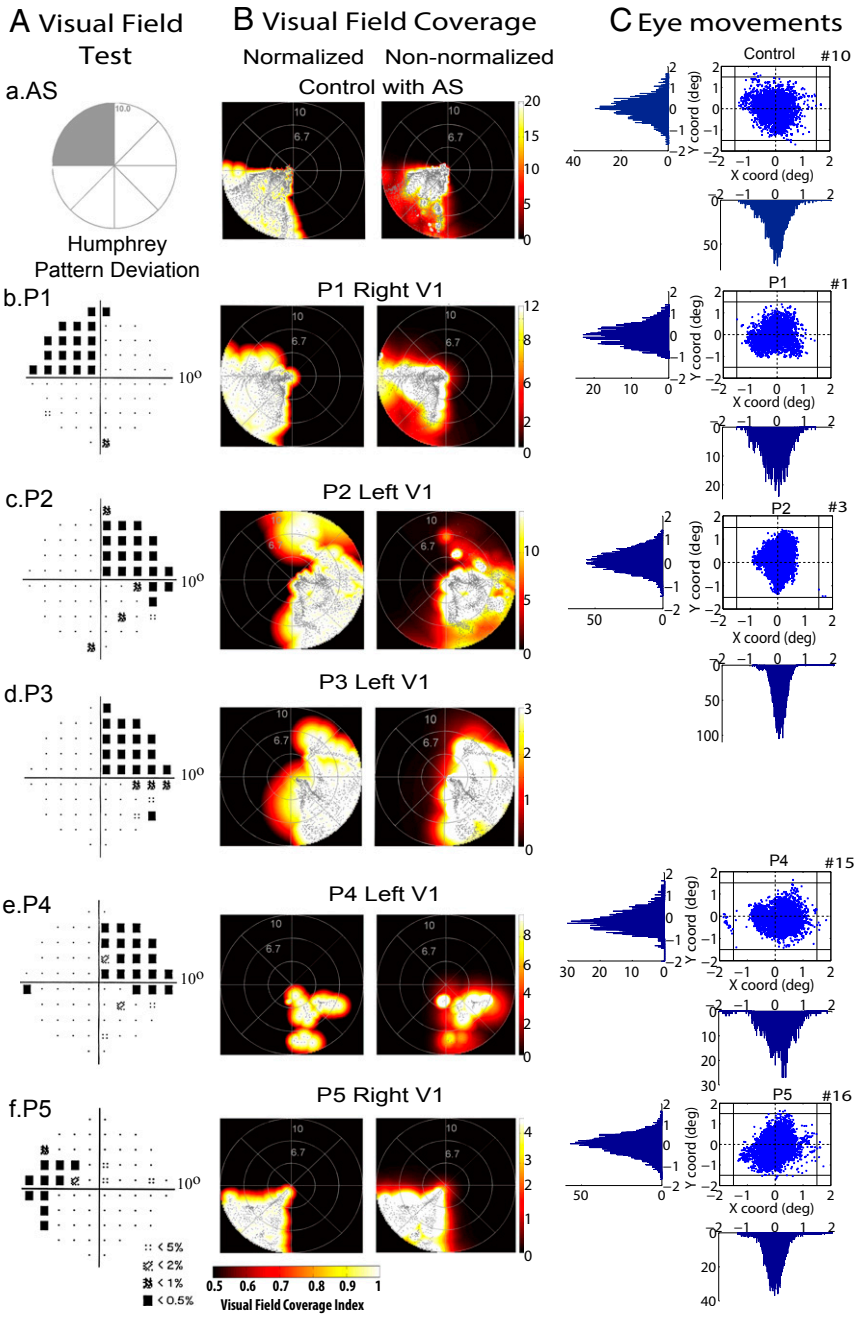

Fig. 2. Perimetry maps versus visual field coverage maps of spared area V1. (*A*) (*a*) Sketch of the visual field indicating the location of the artificial scotoma (shaded gray area). (*b–f*) Pattern deviation probability plots of the 10° Humphrey type (10, 2) visual field test for patients P1, P2, P3, P4, and P5. The small black dots show the locations in the visual field that are normal, and the black squares indicate a visual field defect at a $P < 0.5\%$ level according to the pattern probability plot (meaning that <0.5% of normal subjects would be expected to have such a low sensitivity at this visual field location). Pattern deviation numeric plots for patients P1, P2, P3, and P4 had a visual sensitivity of <−20 dB, indicating absolute visual field scotoma (56), at all visual field locations within the affected quadrants. Black squares outside the affected quadrants had a visual sensitivity of <−10 dB (most still <−20 dB) for these patients. Patient P5 had a visual sensitivity of <−20 dB (absolute scotoma) in all of the black square locations. (*B*) Visual field coverage maps of area V1 for a control subject with AS in the upper left quadrant and for each patient. The color map indicates the maximum pRF amplitude at each visual field location of all of the pRFs covering that location. The pRF centers across all voxels within the spared V1 are plotted with gray dots. In the normalized maps (*Left*), values range between 0 and 1, because the fitted Gaussian model is normalized to 1. In the nonnormalized maps (*Right*), the maximum pRF amplitude of the nonnormalized Gaussian pRFs is plotted. The nonnormalized color map is plotted with the maximum color value taken at the median pRF amplitude across all pRFs (*SI Materials and Methods*) to maintain sensitivity to relatively low values. The V1 coverage maps of patients P1, P2, and P3 overlap significantly with locations of the perimetric map that show an absolute scotoma (black squares with decibel deviations of <−20 dB). Only a few pRFs (~6%) of patient P2's spared-V1 overlap with locations of the perimetric map (black squares) that have a lower decibel deviation, between −10 dB and −20 dB. (*C*) Eye positions plotted at 60 Hz for each subject for one entire session (6.4 min). The number of eye deviations, defined as excursions >1.5° from the fixation point, is indicated next to the graphs with #. Patient P3 was scanned without eye-tracking while performing a task at fixation. All other patients were able to maintain fixation.

organization, similar to control subjects. In particular, the pRF center eccentricity maps (Fig. 1 *C*, *a–c*) show that the foveal representation was in the occipital pole, as expected, and that increasingly anterior locations responded to increasingly eccentric stimuli. In addition, the representation of the visual field in the dorsal spared V1 corresponding to the sighted quadrant extended from the horizontal meridian to the lower vertical meridian, as shown on the pRF polar angle maps (Fig. 1 *B*, *a–c*), similar to controls. Surprisingly, in these patients, the polar angle map shows significant activity in locations ordinarily corresponding to the inferior part of the calcarine (separated by the dotted line; Fig. 1 *B*, *a–c*), a region normally activated by stimuli presented in the superior part of the visual field, where the perimetry shows a dense scotoma (Fig. 2 *A*, *b–d*). We investigated this pattern in more depth, as discussed in the next section.

Patients P4 and P5 exhibited a different pattern. In these patients, the extent of the retinotopic topography of area V1 that was activated was considerably less than would be predicted from the visual field maps. Specifically, for patient P4, the organization of spared area V1 was severely disrupted, and almost the entire dorsal V1, except for a sliver near the lower vertical meridian, was devoid of activity (Fig. 1 *B–D*, *d*). Nevertheless, the perimetry map of this patient closely conforms to a superior quadrantanopia, with only a slight extension below the horizontal meridian. The relatively well-preserved perimetry map of the right lower visual field quadrant (Fig. 2 *A*, *e*) suggests either the presence of sufficient intact dorsal V1 islands to compensate (even though they are not visible on the retinotopic map) or the presence of functional V1-bypassing pathways to higher areas that may have more complete retinotopic coverage maps (35).

Similarly, patient's P5 visual cortex inferior to the calcarine was severely affected, with no visually driven functional activity present in the ventral occipital region as a whole (Fig. 1 *B–D*, *e*). However, this subject shows a sparing along the left upper vertical meridian in the perimetry map (Fig. 2 *A*, *f*). Presumably, preserved visual function in the left upper visual field is mediated by V1-bypassing pathways, likely involving areas beyond V3 (*Discussion*), or perhaps via the contralesional hemisphere (left area V1). We explore this in more details in the next section.

In summary, we observed two different patterns in the five patients that we examined. Patients P1, P2, and P3 had visually driven activity in spared V1 regions that corresponded to dense locations of their perimetric scotoma. In contrast, patients P5 and P4 had intact perimetric maps in locations corresponding to area V1 regions, with an absence of visually driven activity. We analyzed these patterns further using the concept of visual field coverage maps.

Correspondence Between Visual Field Coverage Maps and Perimetric Scotomas. To estimate how the visual field is represented in spared area V1, we superimposed appropriately normalized pRFs arising from all of the spared V1 voxels to derive visual field coverage maps (Fig. 2*B* and *SI Materials and Methods*). The visual field coverage maps define the locations within the visual field that evoke a significant response from voxels within a region of interest (ROI) in the cortex. Determining the degree to which visual field coverage maps match perimetric maps, which indicate the patients' perceptual scotoma, is of interest.

To ensure that the patients' visual field coverage maps are not an artifact of poor pRF estimation caused by the presence of the visual field scotomas, we tested the effect of an "artificial scotoma" (AS) on normal subjects. We measured responses in five control subjects while masking the left superior quadrant of the visual field, thereby simulating a left upper quadrantanopia. As expected, the visual field coverage maps of the right V1 hemisphere in AS controls reveal visually driven activity only for stimuli presented in the left inferior visual field quadrant (Fig. 2 *B*, *a*). No activity was observed in the left upper visual field quadrant in any of the five AS control subjects.

In contrast, the visual field coverage maps of spared V1 in patients P1, P2, and P3, who had a quadrantic visual field defect similar to AS controls, contain pRF centers that extend well beyond the border of the perimetric scotoma into the superior (anopic) visual field quadrant (Fig. 2 *B*, *b–d*). The pRFs, whose centers fall inside the area of the scotoma, belong to voxels at the correct anatomic location, inferior to the calcarine, which do not appear to be grossly ectopic (Fig. 3). Thus, the observed activity likely reflects islands of V1 that were spared or only partially damaged. Interestingly visually driven activity in this spared V1 region is not sufficient to guarantee visual awareness, as measured by standard perimetry.

One possibility is that the blood oxygen level-dependent (BOLD) signal amplitude is lower at V1 locations covering the interior of the scotoma and thus cannot mediate visual perception. However, for patients P1 and P3, the mean amplitude of the pRF centers that fall inside the perimetric scotoma was similar to the mean amplitude of pRF centers located outside the scotoma, as shown in the nonnormalized visual field coverage maps (Fig. 2 *B*, *b* and *d*). In this case, the dense perimetric defect near the horizontal meridian might be explained by injury in downstream extrastriate areas, such as V2/V3 (36, 37), or the interruption of V1 projections to extrastriate areas. In fact, the lesion of these patients involves areas V2v and V3v, supporting the first possibility.

On the other hand, for patient P2, who had an optic radiation lesion, the loss of visual perception cannot be attributed to a lesion downstream from area V1, because the visual cortex remained intact. Responses in ventral areas V2 and V3 overlapped with the area of the scotoma, similar to V1 (Fig. S1*A*). In this case, the nonnormalized visual field coverage maps showed a significantly lower mean amplitude of pRF centers falling inside the scotoma compared with those in the inferior (sighted) quadrant (Fig. 2 *B*, *c* and Fig. S1*A*). Thus, it is possible, at least in principle, that this decreased level of visually driven activity is responsible for the loss of visual perception as measured by perimetry. Interestingly, scattered pRF centers with high amplitude remained inside the scotoma. One possible explanation for this finding is that intact islands of spared, partial axonal tracts in the optic radiation survived after the ischemic event and activate corresponding locations in area V1. Despite being visually driven, however, these islands were unable to mediate visual perception as measured on perimetric maps and cannot be detected even with the relatively sophisticated perimetry mapping methods used here (*SI Materials and Methods*).

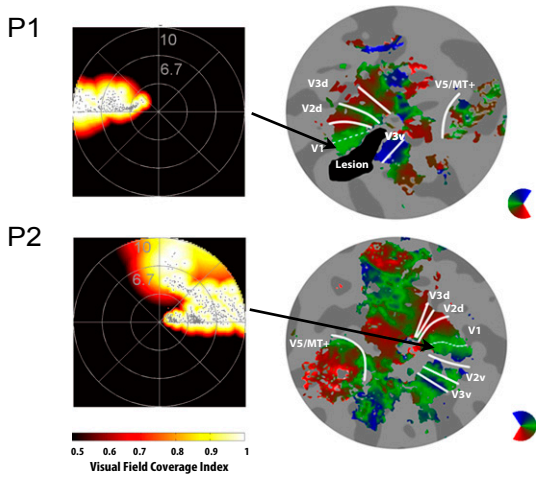

Fig. 3. Anatomic localization of area V1 population receptive fields within the scotoma. (*Left*) Visual field coverage maps obtained from the region of spared V1 inferior to the bottom of the calcarine sulcus (anatomic location of the horizontal meridian) for patients P1 and P2. (*Right*) Anatomic location of the bottom of the calcarine sulcus indicated by a dashed line on the polar angle flat maps. Note that pRFs with centers falling within the scotomatous area in these patients map to the correct anatomic location, inferior to the calcarine (black arrow).

The mismatch between the visual field coverage map and perimetric scotoma does not manifest in the same way in every individual. For example, the visual field coverage of the spared V1 in patient P4 shows pRF centers within the inferior quadrant, outside the visual field scotoma (Fig. 2 *A* and *B*, *e*). In patient P5, a few pRF centers below the horizontal meridian seemed to fall in areas where the perimetry test showed a dense defect, as in patients P1, P3, and P2 (Fig. 2 *A* and *B*, *f*). However, the more striking observation in both these patients is the smaller than expected (based on the perimetry map) activated area in V1. In patient P4, the activation pattern seen in area V1 (Fig. 2 *B*, *e*) was patchy and smaller than expected based on the perimetric map. The visual field coverage map of the right inferior (sighted) quadrant contained significantly fewer pRF centers compared with controls, although the corresponding pRFs cover most, but not all, of the quadrant.

It is possible that pRFs in surviving islands of area V1 enlarged over time, producing a confluent visual field coverage map that partially mediated the residual visual function. However, even taking this into account, the pRF coverage map appeared to miss portions of the visual field where the perimetric map showed normal vision. This finding suggests that part of the residual visual function may be mediated through spared V1-bypassing pathways. In fact, dorsal areas V2 and V3 showed full coverage of the lower visual field quadrant, supporting this hypothesis

(Fig. S1*B*). Similarly, the perimetry map of patient P5 showed a significant area of sparing along the vertical meridian and beyond, within the left upper visual field quadrant (Fig. 2 *A*, *f*). Surprisingly, there was no contralateral V1 activation corresponding to that quadrant, despite the fact that a significant portion of the quadrant was essentially normal on the perimetry map (Fig. 2 *A*, *f*). One possibility is that visual perception near the vertical meridian might arise from V1-bypassing pathways providing direct input to extrastriate areas beyond V3 (35), or perhaps from ectopic V1 activation in the contralesional hemisphere.

The differences in visual field coverage maps between patients and AS controls cannot be explained by eye movements. Subjects were able to maintain fixation within a 1.5° radius from the center of fixation as measured with our eye-tracking system (Fig. 2*C* and *SI Materials and Methods*), except for very occasional excursions beyond this range (Fig. 2). The results remained unchanged after the epochs in which the patients had eye deviations (>1.5°) from the fixation point were removed from the analysis. Patient P3's eye movements were not recorded, but he performed a challenging detection task at fixation, and his performance was always >80% correct. The retinotopic maps of his healthy hemisphere were well organized, suggesting that he did not make large, confounding eye movements. In addition, to ensure intrasubject reproducibility, we repeated the experiment on another day for patients P2 and P5 and confirmed the findings across days. Patients P1, P3, and P4 could not repeat the session; however, we analyzed each scan separately before averaging and confirmed the reliability across different scans obtained on the same day.

In summary, our comparison of perimetric maps and pRF coverage maps of the visual field confirmed the two patterns of mismatch noted in the previous section. In three of the five patients, spared area V1 pRF maps overlapped significantly with the scotoma, suggesting remaining visually responsive islands of V1 that cannot contribute to visual perception, perhaps because of damage to downstream areas or damage to the inputs that they receive from area V1. In the remaining two patients, spared V1 pRF maps failed to completely cover locations that were found to have intact thresholds on perimetry. In these patients, the observed mismatch might indicate the existence of V1-bypassing pathways able to mediate useful vision. The information obtained from pRF analysis complements that obtained by standard perimetry maps, and can be used to further characterize the underlying etiology of cortical visual field defects.

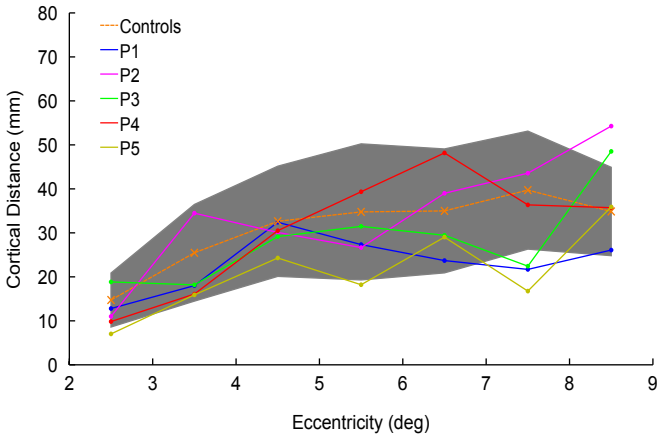

Fig. 4. Cortical distance between the V1 horizontal meridian and dorsal V1/V2 border for patients P1–P5. The cortical distance is calculated by measuring the surface area of seven isoeccentric ROIs (range of eccentricities, 2–9°; bin size, 1°) and dividing by the cortical magnification factor (mm/°) at each eccentricity. The mean cortical distance of the controls (mm) is plotted as an orange dotted line. The gray shaded area indicates the SD (n = 16 hemispheres).

pRF Center Distributions in Spared Area V1 Show at Best Limited Reorganization. A general finding in all five patients was that the retinotopic representation of the spared V1 remained grossly unaffected (Fig. 1). The borders between visual areas, as marked by polar angle reversals, were detected at the expected locations. We measured the cortical distance from the V1 horizontal meridian to the dorsal V1/V2 border along isoeccentricity contours, and plotted it as a function of eccentricity. Plots for all patients were within the range of controls (Fig. 4). Furthermore, the Talairach coordinates at an eccentricity of 8° along the horizontal meridian of V1 and the dorsal V1/V2 border were similar to those of controls (Table S2), and consistent with previous reports (38). In addition, the eccentricity maps exhibited a monotonic progression of phase, as expected (Fig. 1*C*). These results reveal that large-scale retinotopic distortions do not occur; however, the possibility of fine changes in the retinotopic structure of spared V1 cortex cannot be excluded and merits quantitative assessment.

To do so, we compared the distributions of pRF center locations between patients and AS controls. The AS serves as a baseline to control for pRF changes that may arise from reorganization versus simple stimulus deprivation. This control might not always be completely adequate, however, given that partial deafferentiation of the visual pathways may affect the pRFs corresponding to visual field locations that do not belong to the scotoma. Thus, a case-by-case evaluation of whether pRF differences between patients and AS controls are result of partial deafferentiation as opposed to remapping or true reorganization is needed.

pRF center distribution as a function of distance from the scotoma border. In two of the five patients (P1 and P2), the distribution of pRF centers as a function of distance from the horizontal border of the scotoma (elevation) differed significantly from that of AS controls [two-sample Kolmogorov–Smirnov test; significance is reported as $P = a < b$, where b is the value selected to reject the null hypothesis (*Materials and Methods*); P1: $P = 8.09 \times 10^{-63} < 10^{-27}$; P2: $P = 7.62 \times 10^{-42} < 10^{-27}$]. Specifically, pRF centers were seen to cluster near the border of the scotoma, that is, the horizontal meridian (Fig. 5*A*). In fact, in these patients, a number of pRF centers crossed the scotoma border to lie inside the scotoma (i.e., with elevation > 0°), as seen in the visual field coverage maps (Fig. 5*A*, *Insets*). These pRFs belonged to voxels that were not anatomically ectopic but mapped roughly at the correct anatomic location, the lower bank of the calcarine sulcus (Fig. 3). One may then wonder whether they are the reason that pRF centers cluster more strongly near the border of the scotoma in patients compared with AS-controls. However, the distribution of pRFs of the spared dorsal V1, defined by its anatomic location, was also significantly shifted toward the scotoma border, with voxels clustering near the border (0° elevation) (Fig. 5*B*; P1: $P = 8.09 \times 10^{-38} < 10^{-26}$; P2: $P = 8.09 \times 10^{-38} < 10^{-26}$). This finding suggests that the observed shift in the distribution of pRF centers likely corresponds to a slight reorganization of the visual field coverage map in unlesioned portions of area V1 that are located close to the scotoma border, perhaps because of a change in local excitation/inhibition balance as a result of the lesion.

This effect was not seen in every patient. The distribution of pRFs in the dorsal V1 of patient P3 did not show significant clustering near the border of the scotoma compared with AS controls ($P = 1.4 \times 10^{-15} > 10^{-28}$) (Fig. 5*B*). Patients P4 and P5 had fewer voxels with pRFs inside the sighted quadrant compared with AS controls, and P4 also showed a trend toward clustering of pRF centers at the scotoma border, but this did not reach significance under our relatively strict comparison criterion (P4: $P = 1.48 \times 10^{-04} > 10^{-07}$; P5: $P = 9.6 \times 10^{-04} > 10^{-11}$) (Fig. 5*A*). Regardless, the lesions of patients P4 and P5 extended to

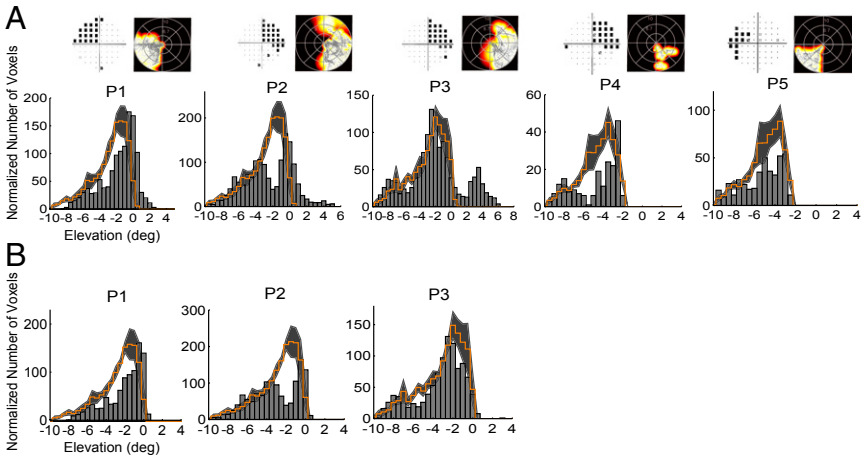

Fig. 5. pRF center distribution as a function of distance from the scotoma border. (*A*) Histograms (gray bars) showing the number of voxels as a function of the pRF center elevation, that is, the distance of the pRF center from the horizontal meridian border of the scotoma (coordinate Y), for patients P1–P5. Units are degrees of visual angle. The mean distribution of voxels in the control subjects with AS is overlaid as a step histogram in orange. To adjust for V1 size, the distributions of the controls were normalized according to the relative size of the retinotopically corresponding V1 regions that were activated in patients versus controls under the full stimulation condition (*SI Materials and Methods*). The shaded area represents the SEM for the control group ($n = 5$). The pRF center elevation distributions of patients P1, P2, and P3 show pRFs within the area of the scotoma (elevation >0), as also shown in the visual field coverage maps (*Insets* and Fig. 2 *B*, *b–d*). However, for patients P1 and P2, there was also a clustering of voxels near the scotoma border. The pRF center elevation distributions of patients P4 and P5 show fewer voxels within the sighted quadrant compared with AS controls and a clustering near the scotoma border for P4, but the effect did not reach significance. The observed differences between these patients and AS controls are likely related to partial deafferentiation of the voxels plotted. (*B*) pRF center elevation distributions of the significantly activated voxels in the anatomically defined intact dorsal V1 of patients P1, P2, and P3. For patients P1 and P2, pRFs clustered significantly near the scotoma border, suggesting reorganization. This effect was not seen in patient P3.

partially involve dorsal V1 or its inputs (Fig. 1 *A*, *d* and *e*), making it difficult to determine whether observed changes are related to true reorganization or to partial deafferentiation.

In summary, these results suggest that in some patients with partial lesions of area V1 or its inputs (here P1 and P2), the pRF centers of spared V1 cortex cluster near the border of the scotoma. This clustering is seen primarily within 1–2° of the scotoma border. The magnitude of the shift is small, suggesting a limited degree of reorganization. One patient (P3) did not exhibit this effect; however, this patient's injury occurred only 6 mo before recruitment, compared with the chronic lesions of the other patients, and we cannot exclude the possibility that time may affect the degree of the observed reorganization. In patients P4 and P5, the observed differences are more likely related to partial deafferentiation or partial injury of the corresponding voxels.

Population receptive field size. We found a larger mean pRF size in the spared V1 area in patients compared with AS controls (Fig. 6). Specifically, the mean pRF size in the spared V1 of patients P1, P2, P4, and P5 was increased by ∼25% compared with AS controls. A larger increase was seen in patient P3, ∼90% compared with AS controls. The pRF size distributions of patients P1, P2, and P3 were significantly shifted toward larger sizes compared with the AS controls ($P = 1.4 \times 10^{-76} < 10^{-63}$, $P = 1.67 \times 10^{-78} < 10^{-70}$, and $P = 1.13 \times 10^{-165} < 10^{-66}$, respectively) (Fig. 6*A*). The same trend was seen for patients P4 and P5, but it did not reach significance ($P = 7.4 \times 10^{-09} > 10^{-39}$ and $P = 1.19 \times 10^{-33} > 10^{-62}$) (Fig. 6*A*). V1 lesions were larger in these patients (Fig. 1 *B*, *d* and *e*), leading to few visually modulated area V1 voxels and thus more measurement variability. In addition, in these patients, the pRFs were located at higher eccentricities, where pRF sizes are larger. In general, the mean pRF size for each patient was greater than the corresponding mean of the distribution of pRF sizes of the AS controls (Table S3).

We examined whether the pRF size increase depends on eccentricity and distance of the voxel from the scotoma border. To do so, we divided voxels in the spared V1 of patients and AS controls into two categories: voxels with pRF centers within 2° of the horizontal scotoma border and voxels with pRF centers >2° from this border, and plotted mean pRF size versus eccentricity (Fig. 6 *B* and *C*). We found that for all patients, mean pRF size was increased for voxels located within 2° of the scotoma border (Fig. 6*B*), with increases of ∼40% for patients P2, P4, and P5; ∼75% for patient P1; and ∼120% for patient P3. For patients P1, P2, P3, and P5, the increase occurred across almost the whole range of eccentricities, whereas for P4, it was more profound for large eccentricities (>6°). In contrast, the mean pRF size of voxels >2° away from the scotoma was more similar in patients P1, P2, P4, and P5 and AS controls (Fig. 6*C*). For P3, the mean pRF size was increased for voxels away from the scotoma as well, but to a lesser degree (∼40%) compared with voxels near the scotoma. The larger increase observed in this patient might be attributed to the relatively recent lesion compared with the other patients, but we cannot exclude the possibility that small eye movements might have affected the pRF size, considering that this patient was not eye-tracked. However, eye movements would be expected to increase pRF size in higher areas in a comparable way as in V1 (39). In patient P3, pRF size in areas V2d and V3d was slightly larger (∼15%) compared with that in AS controls, but the magnitude of the increase was considerably less than observed in area V1 and did not occur for all eccentricities (Fig. S2). Thus, eye movements cannot be the sole explanation for the pRF size increase observed in area V1 of this patient.

In summary, the pRF size distribution in the spared V1 regions of patients with partial quadrantanopia appeared to shift toward larger values compared with the AS controls, particularly near the scotoma border.

Contralesional Hemisphere. Previous reports have suggested that in some cases, residual vision in the blind hemifield might be mediated by visual areas in the intact hemisphere (40–43). It is then possible that after area V1 injury, reorganization might occur in the contralateral, healthy hemisphere. Because in primates, callosal projections are concentrated along the V1/V2 boundary (44), the vertical meridian is the most natural place in the contralesional hemisphere to look for potential reorganization. We compared pRF sizes between the dorsal and ventral V1 and

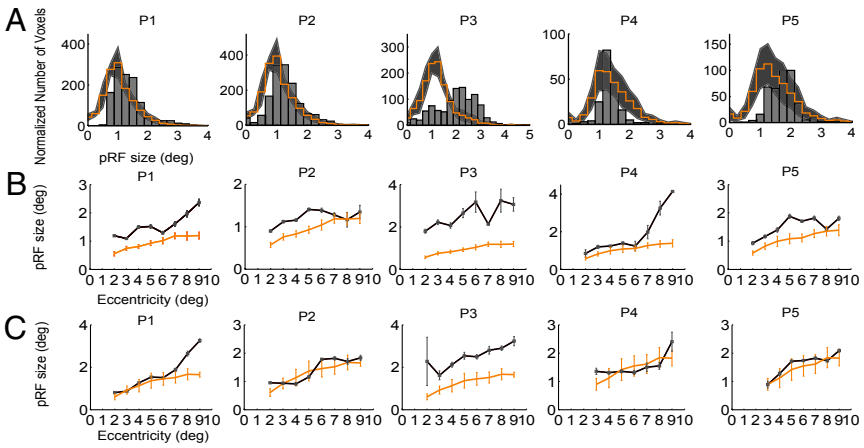

Fig. 6. pRF size in spared V1 areas. (*A*) Histograms of the distribution of pRF size from the spared V1 of all patients (gray bars) compared with the mean distribution of AS controls (orange stairs). The shaded area indicates the SEM across the AS controls. The pRF size distribution of all patients is shifted toward larger pRF sizes compared with the AS controls. (*B*) Mean pRF size versus eccentricity for voxels located near the scotoma border (<2°) in patients (black) and AS controls (orange). The orange error bars indicate the SEM across AS control subjects (n = 5). The gray error bars indicate the SEM across voxels within an eccentricity bin (bin size, 1°) for each patient. Mean pRF size is larger in patients compared with AS controls across eccentricities. pRFs within the area of the scotoma of patients P1, P2, and P3 were not included in the plots; however, results remain the same when these voxels are included. (*C*) Mean pRF size versus eccentricity for voxels located away from the scotoma border (>2°) in patients (black) and AS controls (orange). Mean pRF size was similar in patients P1, P2, P4, and P5, and AS controls across eccentricities, with only P1 having a slightly increased pRF size for eccentricities >7°. For P3, the mean pRF size was larger than that of AS controls for all eccentricities. Eye movements cannot explain the observed differences for patients P1, P2, P4, and P5, given that the distribution of eye movements was similar in patients and controls (Fig. 2*B*) and eye movements would have caused an increase in pRF size at low eccentricities irrespective of distance from the scotoma border. Patient P3 was not eye-tracked, and thus we cannot completely exclude that possibility. However, pRF sizes in areas V2d and V3d did not increase similarly to those in V1, suggesting that eye movements might not be responsible for the large increase observed in V1 (Fig. S2).

between the vertical and horizontal V1 meridians of the hemisphere ipsilateral (contralesional) to the visual field scotoma in patients and in AS controls. Patients P1, P2, P3, and P4 showed no significant difference in mean pRF size between contralesional dorsal and ventral V1 or between vertical and horizontal V1 meridians (Fig. S3); however, the pRF size distribution of the entire contralesional V1 in each patient showed a significant shift to larger pRF sizes in patients P2, P5, and P3 compared with AS controls ($P = 1.63 \times 10^{-64} < 10^{-62}$, $P = 2.55 \times 10^{-167} < 10^{-70}$, and $P = 4.93 \times 10^{-236} < 10^{-63}$ respectively) (Fig. 7*A*). The increase occurred across all eccentricities in patients P3 and P5 and mainly for eccentricities >5° in patient P2 (Fig. 7*B*). Patients P1 and P4 had a pRF size distribution more similar to that of AS controls, with differences that did not reach significance (P1: $P = 8.34 \times 10^{-34} > 10^{-64}$; P4: $P = 7.53 \times 10^{-18} > 10^{-55}$) (Fig. 7*A*); however, these patients had a larger pRF size for eccentricities >7° compared with AS controls (Fig. 7*B*).

Only patient P5 had significantly larger pRFs in the ventral contralesional V1 than in the dorsal contralesional V1, particularly along the upper vertical meridian (Fig. S3). This finding is intriguing, and it is tempting to associate it with the sparing seen in the perimetric map of this patient along the left upper vertical meridian (Fig. 2 *A*, *f*). This association is not certain, however, for several reasons: (*i*) Although larger, patient P5′s pRFs along the vertical meridian crossed only modestly (~1–2°) into the contralateral visual field, and this cannot readily explain the relatively larger sparing seen on perimetric maps; (*ii*) the degree of crossover was commensurate with the size of patient P5′s eye movements (~1.3°); and (*iii*) we cannot completely exclude the possibility that area V1 of the lesioned hemisphere could be mediating visual perception in the spared region seen on visual perimetry while being too weakly visually driven to be evident on the pRF maps.

Discussion

The few published studies of human visual system organization in the setting of area V1 injury are mainly case reports (33, 45). Naturally occurring cortical lesions show considerable variability, making it difficult to draw definite conclusions from isolated case studies. Dilks et al. (33) studied a subject with left upper quadrantanopia after damage to the optic radiation and report significant ectopic activity in area V1 at 6 mo after the ictus. Specifically, activity elicited by stimuli presented in the sighted left lower visual field quadrant mislocalized to V1 regions ordinarily corresponding to the blind left upper quadrant, suggesting the occurrence of large-scale reorganization. Whether the ectopic V1 activity that Dilks et al. reported is the result of reorganization or simply the result of a different pattern of visual input between patient and controls is unclear, however. The authors attempted to control for this by removing stimulation epochs corresponding to the left upper quadrant from their analysis in the controls, but this was not necessarily definitive, because the stimulus was in fact presented there. A more appropriate control would have been to mask the stimulus presentation space in the controls to simulate a quadrantic scotoma (AS condition). Given the high intersubject variability, further studies are needed to characterize how the functional properties of the visual cortex change in the context of injury.

Here we used quantitative pRF analysis (34, 46–48) to study the properties of spared V1 cortex in five patients with chronic postchiasmatic lesions resulting in homonymous visual field quadrantanopia. We derived detailed retinotopic maps and visual field coverage maps of spared area V1 for each patient and made the following observations: (*i*) The spared V1 region of the lesioned hemisphere retained its coarse retinotopic organization, as described previously (35, 45), the V1/V2 border remained stable, and retinotopic maps showed a monotonic progression of phase, as expected; and (*ii*) visual field coverage maps of the spared V1 area generally did not exactly match the area of the dense perimetric scotoma (Fig. 2). Two main patterns of mismatch were identified.

Pattern 1: Visual Field Coverage Maps of Spared-V1 Overlapped Significantly with the Dense Perimetric Scotoma in Three of the Five Patients. pRFs activated inside the scotoma were found in the proper anatomic locations. Thus, in patient P2, whose scotoma

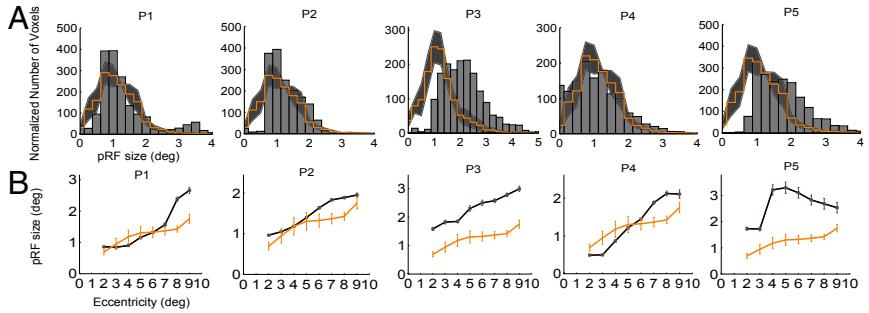

Fig. 7. pRF size of the contralesional V1. (*A*) Histograms of the distribution of pRF sizes from the contralesional V1 of all patients (gray bars) compared with the mean distributions of AS controls (orange stairs). The shaded area indicates the SEM across AS controls ($n = 5$). The distributions show a significant shift to larger pRF sizes for patients P2, P3, and P5. Patients P1 and P4 showed a significant increase in pRF size only for eccentricities >7°. (*B*) Mean pRF size versus eccentricity for voxels in the contralesional V1 of patients (black) and AS controls (orange). The orange error bars indicate the SEM across AS control subjects ($n = 5$). The gray error bars indicate the SEM across voxels within an eccentricity bin (bin size, 1°) for each patient. For patients P1, P2, and P4, pRF size was larger compared with that in AS controls for eccentricities >6–7°. For patients P3 and P5, pRF size was increased across all eccentricities. As shown in Fig. 2*C*, patients P1, P2, P4, and P5 were able to ensure fixation. The amplitude of the eye movements did not differ between patients and controls (Fig. 2*C*), and epochs of significant deviation from fixation were excluded from the analysis; thus, the findings for these patients are unlikely to be attributed to eye movements. Patient P3 was not eye-tracked, however, and even though he was performing a challenging detection task at fixation, in his case we cannot completely exclude that possibility.

resulted from optic radiation injury, residual islands of V1 activity likely received inputs from axonal tracts that are only partially affected by the lesion. These tracts were able to elicit area V1 activity, but were not strong enough to elicit a visual percept (Fig. 2 *B*, *c*). In principle, lack of a percept in the presence of area V1 activity may occur because retinotopically corresponding higher pathways or areas are injured, or because the activity generated in area V1 is too weak or too disorganized to elicit a percept. Patient P2 had no lesion in higher pathways, and so the latter mechanism likely dominates. Given that the pathways from area V1 to higher extrastriate areas were intact and islands of activity were present in the V1 cortex, it is reasonable to view this patient as a prime candidate for visual rehabilitation. In theory, the capacity for recovery would be maximal in the portion of the scotoma that overlaps with the visual field coverage map of area V1.

The two other patients in this category, P1 and P3, had lesions that included ventral areas V2/V3, raising the possibility that the information flow between area V1 and higher extrastriate areas had been cut off. In that event, knowing the region of overlap between the visual field coverage map of area V1 and the scotoma might still be helpful if the projection from spared V1 cortex to extrastriate areas was not completely cut off. Regardless, the region of overlap between a visual field coverage map and the corresponding perimetrically determined visual field scotoma identifies visual field locations that can still generate some level of V1 activity and thus may have greater potential for visual rehabilitation. This strongly suggests that pRF mapping (34, 49) should be incorporated into the design of future visual rehabilitation studies.

Pattern 2: Visual Field Coverage Maps of Spared-V1 Did Not Cover Completely the Sighted Quadrant of the Perimetric Map. Two out of five patients exhibited this pattern of activity. Presumably in this case, residual visual function is mediated by V1-bypassing pathways (as supported by the visual field coverage maps of areas V2/V3 in patient P4; Fig. S1) or perhaps through the contralesional hemisphere. The latter possibility would be supported by a spreading of the pRF coverage map across the vertical meridian, as occurred to some degree in patient P5 (Fig. S3), who exhibited an area of sparing near the vertical meridian in the perimetry map. This occurred to a lesser degree than expected from the area of sparing seen in the perimetric map, however, and thus this hypothesis cannot be verified here; more research is needed. Another possible explanation that we cannot completely exclude here is that in some cases, fMRI mapping might not be sufficiently sensitive to detect weak visually induced activity in early visual areas. This is probably not the complete explanation, however, for several reasons: (*i*) We calculated the BOLD signal-to-noise ratio (SNR) in the areas of interest in all patients and found them to be within the range obtained in controls with AS; (*ii*) the variance explained of voxels corresponding to these visual field locations is within the range obtained in nonvisually responsive areas; and (*iii*) previous studies have shown that BOLD signal amplitude correlates well with visual stimulus perception (50, 51), and in some cases even subthreshold stimuli elicit significant modulation in early visual areas (52).

Do (Spared) Area V1 pRFs Change After the Lesions? pRF measurements provide a way to gauge the degree of reorganization that occurs in early visual areas. The pRF depends on both the size and the position scatter of individual receptive fields within a voxel (53). It thus might be affected by partial deafferentiation of V1 inputs, or may reflect reorganization, that is, sprouting or strengthening of anatomic connections after V1 injury. Incomplete stimulus presentation itself might alter pRF size measurements and result in apparent remapping even in the absence of true reorganization (54). For this reason, changes can be reasonably attributed to cortical reorganization only if they are significantly different than changes observed in controls under the AS condition. Thus, we compared pRF center and size distributions between patients and AS controls.

Does the Position of pRF Centers Reorganize? One important question is whether the pRFs of spared area V1 in patients emerge from voxels that are at the correct anatomic locations versus voxels that are ectopic, suggesting possible reorganization. We have not found voxels with grossly ectopic V1 pRFs in any patient. pRFs fall in approximately correct anatomic locations; that is, pRFs located in the upper visual field belong to voxels located below the calcarine sulcus and vice versa. Finer changes in pRF localization do occur, however.

We found that for two of the five patients (P1 and P2), pRF center elevation (i.e, distance from the scotoma border) distributions differed significantly from that of the AS controls, with clustering near the scotoma border (horizontal meridian). Moreover, this occurred even when we restricted the analysis to the intact part of V1 that corresponds to a normal perimetry (dorsal V1; Fig. 5*B*). This suggests that for these patients, some pRF centers shift their location over short distances to locations near the scotoma border, supporting the notion of reorganization. A

possible mechanism behind this shift is enhancement of surviving single-cell pRFs in voxels near the border of the scotoma after injury, perhaps via a change in the balance of inhibition versus excitation (27–31). The magnitude of the shift is on average only 1°, consistent with at most a limited degree of reorganization.

In contrast, patients P4 and P5 exhibited patchy activation of spared V1. The difference in pRF center distributions between these patients and AS controls may be the result of partial deafferentiation. The remaining patient, P3, had similar pRF center location distributions as AS controls. A possible important difference in this patient is that V1 injury occurred only 6 mo before recruitment, whereas all other patients had been lesioned for years. None of the patients who participated in this study, including the two patients with optic radiation lesions, had ectopic pRF centers over distances comparable to those suggested by Dilks et al. (33).

Does pRF Size Change in Spared-V1 Cortex? pRF size measurements in the spared V1 cortex of patients showed pRF size increases of ∼25% for patients P1, P2, P4, and P5 and ∼90% for patient P3 compared with AS controls. The pRF size difference reached ∼40% for patients P2, P4, and P5, ∼75% for patient P1, and ∼120% for patient P3 near (<2°) the scotoma border, whereas it was correspondingly smaller far (>2°) from the scotoma border (Fig. 6 *B* and *C*). As mentioned earlier, this may stem from decreased inhibition in the area surrounding the lesion (21), or perhaps because subcortical inputs from LGN or the pulvinar may reorganize via sprouting of cortical axons (55) and contribute to the activation of area V1 areas surrounding the lesion.

pRF size in area V1 of the intact hemisphere also increased in patients compared with healthy AS controls. The relative magnitude of the increase was ∼20% for patient P2 and ∼90% for patients P3 and P5. pRFs for patients P1 and P4 increased by ∼30% but only for eccentricities 6–10°. The relative increase in pRF size seen in the contralesional hemisphere may be attributed to loss of input from interhemispheric connections (40–42), although the expectation that these would affect mainly pRFs along the vertical meridian is not well born out.

Conclusions

Although each patient is unique, several themes emerge from our study:

1. Area V1 displays at best a limited degree of reorganization in adult humans with homonymous visual field defects due to postchiasmatic lesions of the visual pathway.
2. This reorganization is manifested in some patients by a small shift in the pRF centers toward the border of the scotoma and in most patients by a slight increase in V1 pRF sizes near the border of the scotoma, as well as in the V1 of the contralesional hemisphere. Finding ways to further expand pRF size in these patients may increase coverage of the visual field defect, inducing recovery.
3. Importantly, pRF measurements in patients with cortical lesions yield information on the functional properties of spared visual cortex that complements the information provided by standard perimetry maps.
4. We identified two different patterns of mismatch between responses in early visual areas and visual perception as measured by perimetry mapping, and examined possible underlying mechanisms.
5. Understanding how surviving visual areas process visual information post-lesion could potentially help guide visual rehabilitation efforts to induce recovery. Future studies of this patient population incorporating pRF measurements are clearly warranted to improve understanding of visual processing in the context of injury.

Materials and Methods

Patients. Four adult patients (age 27–64 y; two females and two males) with visual cortical lesions were recruited at the Center for Ophthalmology of the University Clinic in Tuebingen. One patient (male, age 33 y) was recruited at the Center for Advanced MR Imaging at Baylor College of Medicine. Four of the participants had homonymous visual field defects as a result of ischemic or hemorrhagic stroke at 7–10 y before enrollment in this study, and one patient had sustained an ischemic stroke at 0.5 y before recruitment (Table S1). Nine participants (age 26–65 y; eight males and one female) were recruited as controls. All patients had normal or corrected-to-normal visual acuity. The experiments were approved by the Ethical Committee of the Medical Faculty of the University of Tuebingen and the Institutional Review Board of Baylor College of Medicine.

Scanning. At least two T1-weighted anatomic volumes and a minimum of five fMRI scans were acquired for each patient and averaged to increase the SNR.

Stimuli. The patients were presented with moving square-checkerboard bars that traveled sequentially in eight different directions spanning a circular aperture with a radius of 11.25° around the fixation point. The bar width was 1.875°, and it was moved in a step of half its size (0.9375°) at each image volume acquisition (repetition time, 2 s). Five control subjects were asked to participate in a second session, during which an isoluminant mask was placed in the upper left quadrant of the visual field. The mask covered the area of the stimulus and created an AS.

Data Analysis. Data analysis was performed in MATLAB using the mrVista toolbox (http://white.stanford.edu/software/). Reliable pRF measurements and visual field coverage maps were derived using the direct isotropic Gaussian pRF method (Fig. S5) (34).

Normalization of pRF Center Voxel Distributions. To test for significant differences between individual patients and the mean distribution from controls (38), we normalized the distributions derived from the AS controls separately for each patient. To do so, we scaled these distributions by the ratio of active spared voxels in V1 of each patient divided by the number of active voxels in the retinotopically corresponding V1 regions of the control subjects during full stimulation (i.e., without AS).

Statistical Analysis. We used a two-sample Kolmogorov–Smirnov test to compare pRF center locations and size distributions between the patients and AS controls. The significance level selected to reject the null hypothesis (same distributions) was estimated by comparing each of the control distributions with the mean control distribution. The minimum P value of these comparisons was then used to test for significance differences in the mean distribution between patients and controls. We report significance as $P = a < b$, where b is the value selected to reject the null hypothesis.

Detailed descriptions of the methodology used in this study are provided in *SI Materials and Methods*.

ACKNOWLEDGMENTS. We thank Natalia Zaretskaya and Andreas Bartels for their help with MRI scanning and eye-tracking. This work was supported by National Eye Institute Grants R01 EY019272 and R01 EY024019, Department of Defense Contract W81XWH-08-2-0146, a Howard Hughes Medical Institute Early Career Award (to S.M.S.), the Deutsche Forschungsgemeinschaft, the Plasticise Consortium (Project HEALTH-F2-2009-223524), a McNair Foundation award (to T.D.P.), a McNair Medical Institute award and a Fight for Sight grant (to T.D.P.), and the Max Planck Society.

1. Wandell BA, Smirnakis SM (2009) Plasticity and stability of visual field maps in adult primary visual cortex. *Nat Rev Neurosci* 10(12):873–884.
2. Kaas JH, et al. (1990) Reorganization of retinotopic cortical maps in adult mammals after lesions of the retina. *Science* 248(4952):229–231.
3. Chino YM, Kaas JH, Smith EL, 3rd, Langston AL, Cheng H (1992) Rapid reorganization of cortical maps in adult cats following restricted deafferentation in retina. *Vision Res* 32(5):789–796.
4. Chino YM, Smith EL, 3rd, Kaas JH, Sasaki Y, Cheng H (1995) Receptive-field properties of deafferentated visual cortical neurons after topographic map reorganization in adult cats. *J Neurosci* 15(3 Pt 2):2417–2433.
5. Gilbert CD, Wiesel TN (1992) Receptive field dynamics in adult primary visual cortex. *Nature* 356(6365):150–152.
6. Schmid LM, Rosa MG, Calford MB, Ambler JS (1996) Visuotopic reorganization in the primary visual cortex of adult cats following monocular and binocular retinal lesions. *Cereb Cortex* 6(3):388–405.
7. Calford MB, Schmid LM, Rosa MG (1999) Monocular focal retinal lesions induce short-term topographic plasticity in adult cat visual cortex. *Proc Biol Sci* 266(1418):499–507.
8. Baker CI, Dilks DD, Peli E, Kanwisher N (2008) Reorganization of visual processing in macular degeneration: Replication and clues about the role of foveal loss. *Vision Res* 48(18):1910–1919.

9. Baker CI, Peli E, Knouf N, Kanwisher NG (2005) Reorganization of visual processing in macular degeneration. *J Neurosci* 25(3):614–618.
10. Giannikopoulos DV, Eysel UT (2006) Dynamics and specificity of cortical map reorganization after retinal lesions. *Proc Natl Acad Sci USA* 103(28):10805–10810.
11. Schumacher EH, et al. (2008) Reorganization of visual processing is related to eccentric viewing in patients with macular degeneration. *Restor Neurol Neurosci* 26(4-5):391–402.
12. Dilks DD, Baker CI, Peli E, Kanwisher N (2009) Reorganization of visual processing in macular degeneration is not specific to the "preferred retinal locus." *J Neurosci* 29(9): 2768–2773.
13. DeAngelis GC, Anzai A, Ohzawa I, Freeman RD (1995) Receptive field structure in the visual cortex: Does selective stimulation induce plasticity? *Proc Natl Acad Sci USA* 92(21):9682–9686.
14. Murakami I, Komatsu H, Kinoshita M (1997) Perceptual filling-in at the scotoma following a monocular retinal lesion in the monkey. *Vis Neurosci* 14(1):89–101.
15. Horton JC, Hocking DR (1998) Monocular core zones and binocular border strips in primate striate cortex revealed by the contrasting effects of enucleation, eyelid suture, and retinal laser lesions on cytochrome oxidase activity. *J Neurosci* 18(14): 5433–5455.
16. Sunness JS, Liu T, Yantis S (2004) Retinotopic mapping of the visual cortex using functional magnetic resonance imaging in a patient with central scotomas from atrophic macular degeneration. *Ophthalmology* 111(8):1595–1598.
17. Smirnakis SM, et al. (2005) Lack of long-term cortical reorganization after macaque retinal lesions. *Nature* 435(7040):300–307.
18. Masuda Y, Dumoulin SO, Nakadomari S, Wandell BA (2008) V1 projection zone signals in human macular degeneration depend on task, not stimulus. *Cereb Cortex* 18(11): 2483–2493.
19. Baseler HA, et al. (2011) Large-scale remapping of visual cortex is absent in adult humans with macular degeneration. *Nat Neurosci* 14(5):649–655.
20. Eysel UT, Schmidt-Kastner R (1991) Neuronal dysfunction at the border of focal lesions in cat visual cortex. *Neurosci Lett* 131(1):45–48.
21. Eysel UT, Schweigart G (1999) Increased receptive field size in the surround of chronic lesions in the adult cat visual cortex. *Cereb Cortex* 9(2):101–109.
22. Eysel UT, et al. (1999) Reorganization in the visual cortex after retinal and cortical damage. *Restor Neurol Neurosci* 15(2-3):153–164.
23. Zepeda A, Vaca L, Arias C, Sengpiel F (2003) Reorganization of visual cortical maps after focal ischemic lesions. *J Cereb Blood Flow Metab* 23(7):811–820.
24. Schweigart G, Eysel UT (2002) Activity-dependent receptive field changes in the surround of adult cat visual cortex lesions. *Eur J Neurosci* 15(10):1585–1596.
25. Payne BR, Lomber SG (2002) Plasticity of the visual cortex after injury: What's different about the young brain? *Neuroscientist* 8(2):174–185.
26. Yinon U, Shemesh R, Arda H, Dobin G, Jaros PP (1993) Physiological studies in deafferented visual cortex cells of cats following transplantation of fetal xenografts from the rat's cortex. *Exp Neurol* 122(2):335–341.
27. Rumpel S, et al. (2000) Lesion-induced changes in NMDA receptor subunit mRNA expression in rat visual cortex. *Neuroreport* 11(18):4021–4025.
28. Mittmann T, Eysel UT (2001) Increased synaptic plasticity in the surround of visual cortex lesions in rats. *Neuroreport* 12(15):3341–3347.
29. Barmashenko G, Eysel UT, Mittmann T (2003) Changes in intracellular calcium transients and LTP in the surround of visual cortex lesions in rats. *Brain Res* 990(1-2): 120–128.
30. Yan L, et al. (2012) Changes in NMDA-receptor function in the first week following laser-induced lesions in rat visual cortex. *Cereb Cortex* 22(10):2392–2403.
31. Imbrosci B, Neubacher U, White R, Eysel UT, Mittmann T (2013) Shift from phasic to tonic GABAergic transmission following laser-lesions in the rat visual cortex. *Pflugers Arch* 465(6):879–893.
32. Zhang X, Kedar S, Lynn MJ, Newman NJ, Biousse V (2006) Natural history of homonymous hemianopia. *Neurology* 66(6):901–905.
33. Dilks DD, Serences JT, Rosenau BJ, Yantis S, McCloskey M (2007) Human adult cortical reorganization and consequent visual distortion. *J Neurosci* 27(36):9585–9594.
34. Dumoulin SO, Wandell BA (2008) Population receptive field estimates in human visual cortex. *Neuroimage* 39(2):647–660.
35. Schmid MC, Panagiotaropoulos T, Augath MA, Logothetis NK, Smirnakis SM (2009) Visually driven activation in macaque areas V2 and V3 without input from the primary visual cortex. *PLoS ONE* 4(5):e5527.
36. Horton JC, Hoyt WF (1991) Quadrantic visual field defects: A hallmark of lesions in extrastriate (V2/V3) cortex. *Brain* 114(Pt 4):1703–1718.
37. Slotnick SD, Moo LR (2003) Retinotopic mapping reveals extrastriate cortical basis of homonymous quadrantanopia. *Neuroreport* 14(9):1209–1213.
38. Dougherty RF, et al. (2003) Visual field representations and locations of visual areas V1/2/3 in human visual cortex. *J Vis* 3(10):586–598.
39. Levin N, Dumoulin SO, Winawer J, Dougherty RF, Wandell BA (2010) Cortical maps and white matter tracts following long period of visual deprivation and retinal image restoration. *Neuron* 65(1):21–31.
40. Ptito M, Dalby M, Gjedde A (1999) Visual field recovery in a patient with bilateral occipital lobe damage. *Acta Neurol Scand* 99(4):252–254.
41. Raninen A, Vanni S, Hyvärinen L, Näsänen R (2007) Temporal sensitivity in a hemianopic visual field can be improved by long-term training using flicker stimulation. *J Neurol Neurosurg Psychiatry* 78(1):66–73.
42. Henriksson L, Raninen A, Näsänen R, Hyvärinen L, Vanni S (2007) Training-induced cortical representation of a hemianopic hemifield. *J Neurol Neurosurg Psychiatry* 78(1):74–81.
43. Reitsma DC, et al. (2013) Atypical retinotopic organization of visual cortex in patients with central brain damage: congenital and adult onset. *J Neurosci* 33(32):13010–13024.
44. Hubel DH, Wiesel TN (1967) Cortical and callosal connections concerned with the vertical meridian of visual fields in the cat. *J Neurophysiol* 30(6):1561–1573.
45. Baseler HA, Morland AB, Wandell BA (1999) Topographic organization of human visual areas in the absence of input from primary cortex. *J Neurosci* 19(7):2619–2627.
46. Amano K, Wandell BA, Dumoulin SO (2009) Visual field maps, population receptive field sizes, and visual field coverage in the human MT+ complex. *J Neurophysiol* 102(5):2704–2718.
47. Harvey BM, Dumoulin SO (2011) The relationship between cortical magnification factor and population receptive field size in human visual cortex: Constancies in cortical architecture. *J Neurosci* 31(38):13604–13612.
48. Winawer J, Horiguchi H, Sayres RA, Amano K, Wandell BA (2010) Mapping hV4 and ventral occipital cortex: The venous eclipse. *J Vis* 10(5):1.
49. Lee S, Papanikolaou A, Logothetis NK, Smirnakis SM, Keliris GA (2013) A new method for estimating population receptive field topography in visual cortex. *Neuroimage* 81: 144–157.
50. Boynton GM, Demb JB, Glover GH, Heeger DJ (1999) Neuronal basis of contrast discrimination. *Vision Res* 39(2):257–269.
51. Avidan G, et al. (2002) Contrast sensitivity in human visual areas and its relationship to object recognition. *J Neurophysiol* 87(6):3102–3116.
52. Watanabe M, et al. (2011) Attention, but not awareness, modulates the BOLD signal in the human V1 during binocular suppression. *Science* 334(6057):829–831.
53. Haak KV, Cornelissen FW, Morland AB (2012) Population receptive field dynamics in human visual cortex. *PLoS ONE* 7(5):e37686.
54. Pettet MW, Gilbert CD (1992) Dynamic changes in receptive-field size in cat primary visual cortex. *Proc Natl Acad Sci USA* 89(17):8366–8370.
55. Rose JE, Malis LI, Kruger L, Baker CP (1960) Effects of heavy, ionizing, monoenergetic particles on the cerebral cortex, II: Histological appearance of laminar lesions and growth of nerve fibers after laminar destructions. *J Comp Neurol* 115:243–255.
56. Heijl A, Patella VM, Bengtsson B (2012) *The Field Analyzer Primer: Effective Perimetry* (Carl Zeiss Meditec, Dublin, CA), 4th Ed.